Arch. Mech., 34, 5-6, pp. 553-562, Warszawa 1982

Conditionally sampled measurements of coherent structures in the wall region of a turbulent boundary layer

L. BOGUSŁAWSKI (POZNAŃ), K. KRISHNA PRASAD, J. M. BESSEM and C. NIEUWVELT (EINDHOVEN)

FLOW visualization studies and conditional sampling techniques have established several features of these structures, like a slow retardation of the flow followed by a fast acceleration, and the fact that periods of fast acceleration coincide with periods of intense turbulent activity. In this paper we describe a detection technique that incorporates the both features mentioned above. A few characteristic results obtained are compared with other techniques. It is shown that a sharper description of the events is possible with the present technique.

Studia nad wizualizacją przepływów i techniki próbkowania warunkowego pozwoliły ustalić szereg własności struktur koherentnych, takie jak powolne opóźnienia przepływów, po których następują gwałtowne przyspieszenia, jak również fakt, że okresy gwałtownych przyspieszeń pokrywają się z okresami intensywnej turbulencji. W pracy opisano technikę detekcji uwzględniającą oba powyższe zjawiska. Kilka charakterystycznych wyników otrzymanych w ten sposób porównano z rezultatami uzyskanymi innymi drogami. Pokazano, że za pomocą tej metody uzyskać można dokładniejszy opis zjawisk.

Исследования визуализации течений и техники условных проб позволили установить ряд свойств когерентных структур, таких как медленное запаздывание течений, после которых наступает внезапное ускорение, как тоже факт, что периоды внезапных ускорений совпадают с периодами интенсивной турбулентности. В работе описана техника детекции, учитывающая оба вышеупомянутые явления. Несколько характеристических результатов, полученных таким образом, сравнены с результатами, полученными другим путем. Показано, что при помощи этого метода можна получить более точное описание явлений.

1. Introduction

IN THIS PAPER we restrict our study to coherent structures in the wall region of a turbulent boundary layer. Flow visualization studies and conditional sampling techniques have established four principal features of these structures:

a) a slow retardation of the flow followed by a fast acceleration,

b) the periods of fast accelerations coincide with periods of intense turbulent activity,

c) the periods of b) account for a substantial proportion of the turbulent shear stress; and

d) there exists a marked increase in v-velocities during the ejection periods which are part of the so-called burst cycle.

Over the years many schemes have been devised to detect these structures. Some of the more important characteristics of a few of these schemes are summarized in Table 1.

Table 1. Summary of some coherent structure detection methods.

	Reference	Method of detection	Remarks
1	RAO *et al.* [6]	analog band pass filtering technique	period of detected events $TU_\infty/\delta = 3.6$ to 6 for $y^+ = 30$ to 1000.
2	WILLMARTH and LU [11]	if $\hat{u}' < TL$ detection occurs	large peak of $\overline{uv}$ associated with local minimum of u'.
3	LU and WILLMARTH [4]	quadrant analysis of $\overline{uv}$ signal	time period of detected events $TU_\infty/\delta = 5$, no difference in distribution of height of $\overline{uv}$ peaks for accepted and not accepted events.
4	BRODKEY *et al.* [2]	quadrant analysis of $\overline{uv}$ signal	time period of $TU_\infty/\delta = 3.0$ for $y^+ = 10$ to 45.
5	UEDA and HINZE [7]	analog band pass filtering technique	period of detected events $TU_\infty/\delta = 4.7$ for $y^+ < 9$ and $TU_\infty/\delta = 2.4$ for $y^+ > 20$.
6	BLACKWELDER and KAPLAN [1]	if $(\widehat{u^2} - \hat{u}^2) > ku_{rms}^2$ for $k > 0.9$ detection occurs	time of burst cycle $TU_\infty/\delta = 2.8$, method detects only the most intense bursts, for $k = 1.2$ period of detected events $TU_\infty/\delta = 10$.
7	WALLACE *et al.* [9]	slope criterion for every detected pattern	length of accepted pattern $TU_\infty/\delta = 3.31$ for $y^+ = 15$, very flat minimum in the conditionally-averaged pattern.

The schemes are based on the hypothesis that it is sufficient to use one of the features mentioned above since they are all presumed to belong to the same cycle of events.

The problem with the approach is that the events to be detected are buried in background turbulence. To minimize the interferences from the latter, the raw signal is smoothed by passing it through a filter before applying the detection criterion. The criterion detects either feature a) by working directly on the smoothed signal (WILLMARTH and LU, [11]) or feature b) by looking at a signal constructed from the difference between the raw signal and the smoothed signal. The number of detections obtained from such schemes is a function of two parameters — one describing the characteristics of the filter and the second associated with the threshold level.

In this paper we describe a detection technique that incorporates both features a) and b). A few characteristic results obtained from this techniques are compared with two other techniques. It is shown that a sharper description of the events is possible with the present technique.

2. The detection technique

Two sets of data were analyzed during the course of the work—one taken by VAN DE VEN [8] in a small wind tunnel and the second obtained in a new tunnel, specially for this work. Some of the pertinent details of the two sets are summarized in Table 2. The measurements in both cases were taken by a constant temperature hot wire anemometer with a single tungsten wire probe of diameter 2.5×10^{-6} m.

Table 2. Some details about the data sets.

	Set I	Set II
Free Stream Velocity, m/s	7.1	5.0
R_θ	2100	2000
y^+	15	11
Local Velocity, m/s	3.4	1.7
δ, mm	35	49
u^*, m/s	0.32	0.21

The elements of the data acquisition system are usual for the class of work described here. It consisted of recording the signal on a magnetic tape, digitizing it at 5 kHz in an A/D converter and storing it on a disc for subsequent processing on a Burroughs B7700 digital computer.

As pointed out earlier, the detection technique developed uses features a) and b) of Sect. 1. The detection technique itself consist of four steps:

i) smoothing the normalized fluctuating component of the signal with a moving averaging technique,

ii) identifying a set of patterns as consisting of those portions of the signal that correspond to accelerations,

iii) calculating the "energy" associated with the accelerations above; and

iv) lastly, calculating the "energy" associated with the part of the signal that was "lost" due to filtering during the periods of accelerations of ii).

These lead to the definition of a pattern indicator function

$$F_p(t) = E_{\text{tot},i} I_p(t),$$

where $I_p(t)$ is an intermittency function. The idea of the technique is illustrated in Fig. 1. The definitions and some additional details are given in the block diagram of Fig. 2.

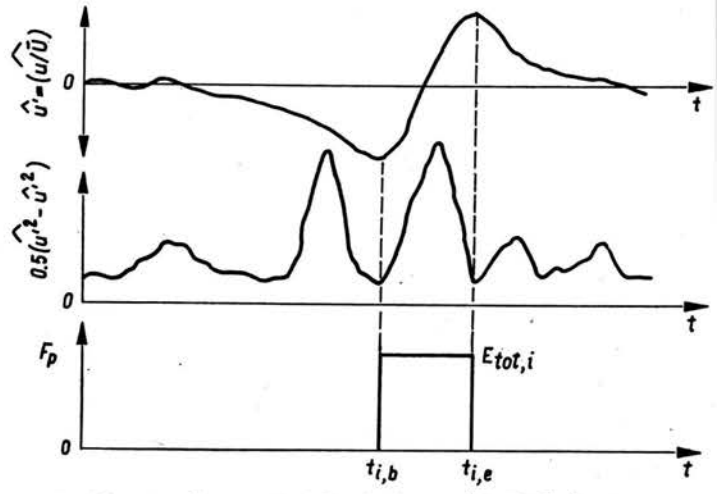

FIG. 1. Typical example of a pattern in smoothed signal, the associated high frequency part and the derived pattern indicator function.

A threshold level, k_a, operates on $F_p(t)$ for classifying patterns into acceptable and non-acceptable ones.

Conditional averaging technique is used for recovering the accepted patterns. Two types of normalization were adopted:

a) one-point normalization based on the minimum point of the accepted pattern; the recovered pattern is displayed on a natural time scale; and

b) two-point normalization based on the minimum as well as maximum points of the pattern; the recovered pattern in this case is displayed on an artificial time scale (t^+).

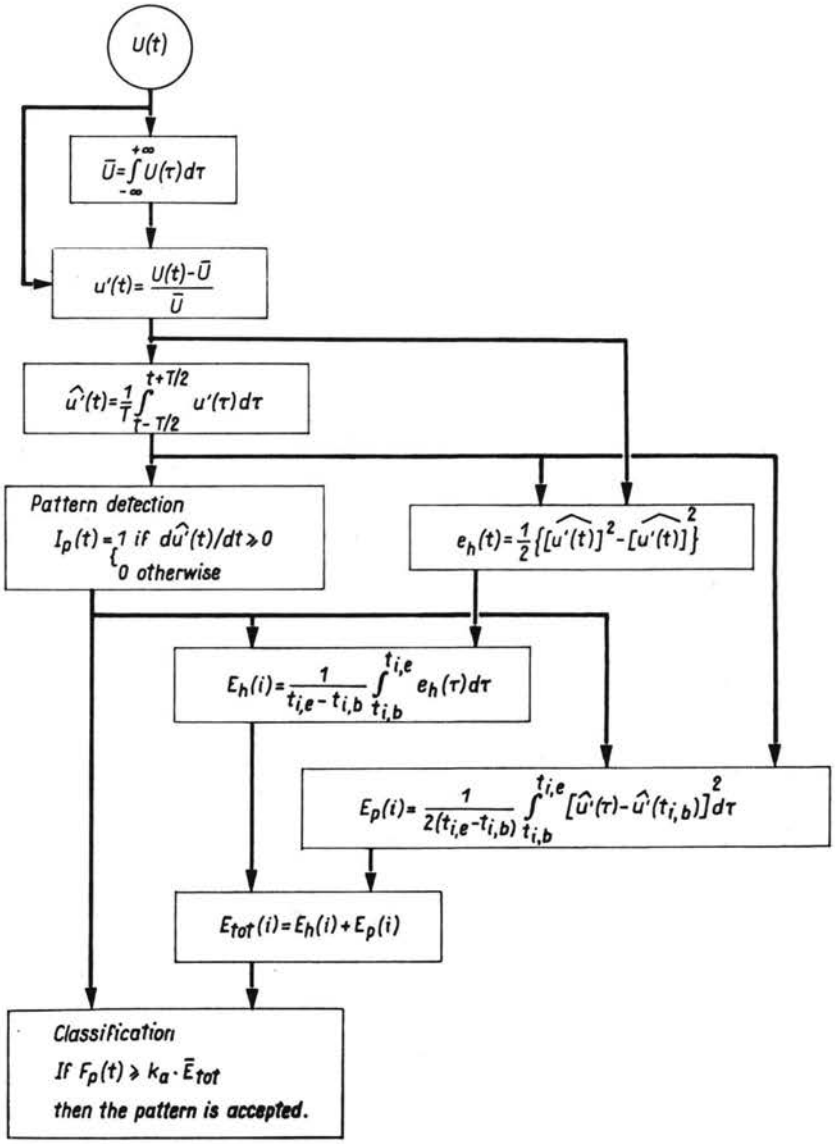

FIG. 2. Block diagram showing the pattern recognition program.

3. Results

As is evident from the description of the technique, the number of accepted patterns depends on the cutoff frequency, f_e, of the filter (defined as $1/T$ where T is the window width employed in the moving averaging technique) and the threshold level k. Figure 3 shows the number of pattern recognitions (as obtained after step (ii) of the procedure) as a function of f_e for a random signal as well as a turbulent signal. The random signal does not show any preferred frequency of filtering. On the other hand, the turbulent signal shows that below certain frequencies (corresponding to point A) we are likely to lose vital information. Thus the filter cutoff frequencies should be larger than about 200 Hz.

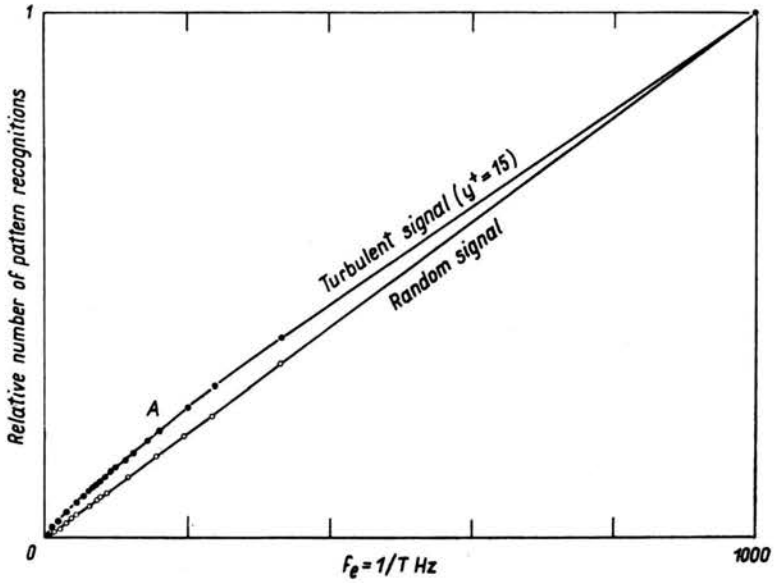

FIG. 3. Number of recognized patterns in the turbulent signal and in the random signal as a function of the cutoff frequency in the moving averaging procedure ($\hat{u}(t) = 1/T \cdot \int_{t-T/2}^{t+T/2} u(\tau)d\tau$).

Figure 4 shows the number of accepted patterns as a function of the threshold level, k for both signals (see the upper curves in Fig. 4). The actual choice of k was based on an examination of the derivative of this function (see the lover curves in Fig. 4). While there is still some noise in these latter curves, it is possible, by examining a number of such curves obtained from different parts of the same signal, to identify a common point where a significant jump in slope occurs.

Based on this procedure, the number of accepted patterns is found leading to the average time interval between two successive patterns. Figure 5 shows a plot of this time interval against f_e. This plot reveals a clear asymptote for both signals and the nondimensional time corresponding to this asymptote is 2.8 ± 0.2.

Two-point normalized, conditionally-averaged accepted velocity patterns and the

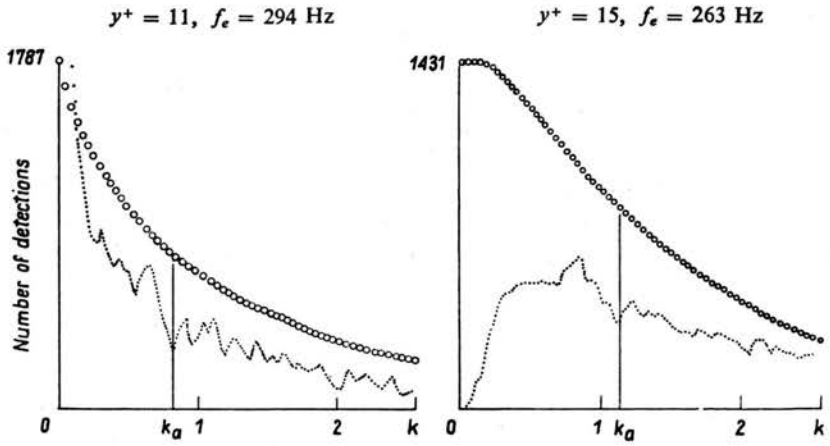

Fig. 4. Number of detected events and the probability density versus height of the pattern indicator function.

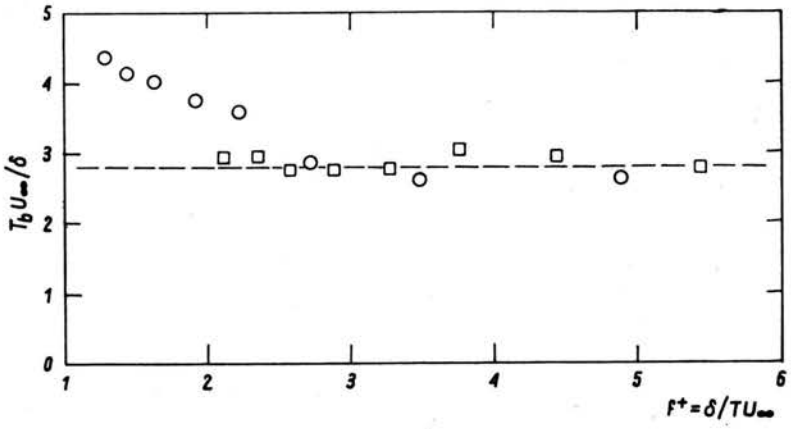

FIG. 5. The dimensionless time interval between the accepted events as a function of the cutoff frequency in the moving averaging procedure. ○ — $y^+ = 15$, □ — $y^+ = 11$.

mean high frequency kinetic energy associated with these patterns are shown in Fig. 6a. These show the usual behaviour of a slow deceleration followed by a rather strong acceleration characteristically observed with typical burst patterns. The acceleration region is strongly correlated with a peak in the high frequency kinetic energy distributions. A similar picture has been drawn for the patterns that were not accepted by the detection scheme in Fig. 6b. Amplitudes of deceleration and acceleration are smaller and, moreover, the peak in high frequency kinetic energy during the acceleration period is the same as that of background turbulence. Finally, Fig. 7 shows the conditionally-averaged profiles obtained by using the smoothed signal only for defining the pattern indicator function. The number of accepted patterns in this case is reduced by about 15%, but the conditionally-averaged profiles remain similar to those in Fig. 6a. This means that the peak in the high frequency kinetic energy is not produced by the detection technique but is a genuine property of the original signal.

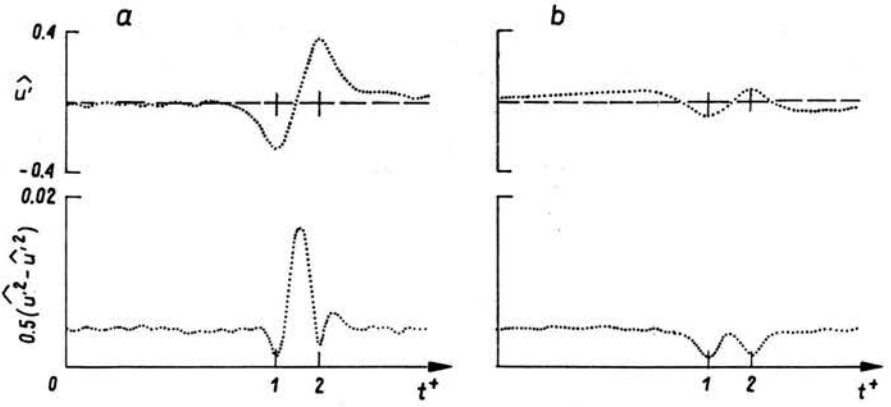

Fig. 6. Comparison of the conditionally averaged patterns a) for the accepted events and b) for the not accepted events.

$y^+ = 11$, $f_e = 294$ Hz, $Tu^{*2}/\nu = 10$.

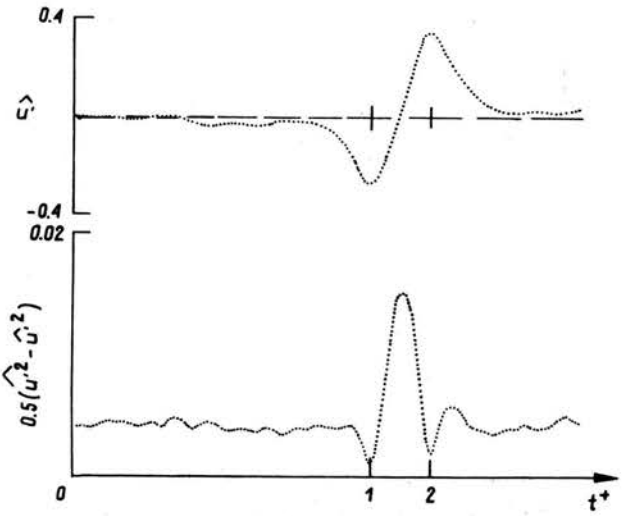

FIG. 7. Conditionally averaged patterns, detection without the high frequency part in the pattern indicator function.

$y^+ = 11$, $f_e = 294$ Hz.

Finally, we compare the results obtained from the present technique with those from the techniques of WILLMARTH and LU [11] and BLACKWELDER and KAPLAN [1]. Two tests were employed for purposes of comparison. The first consisted in requiring that all the schemes produce the same total number of accepted patterns, i.e. $T^+ = 2.8$. Figure 8 shows the one-point conditionally-averaged patterns obtained from the three methods. A striking feature of this figure is that all the methods produce peaks in the high frequency kinetic energy during the acceleration phase of the velocity profiles. However, the velocity

profiles produced by Willmarth and Lu, and Blackwelder and Kaplan are unacceptable in our opinion. The former uses a procedure of picking events on the basis of large negative peaks and as such the conditionally-averaged profiles show very small positive peaks. The latter, being based on large high frequency kinetic energy, (which has been shown to be a characteristic property of the original signal and always associated with the acceleration phase of the smoothed signal) not only misses the deceleration phase completely but also produces rather small peak-to-peak amplitude in the velocity profiles.

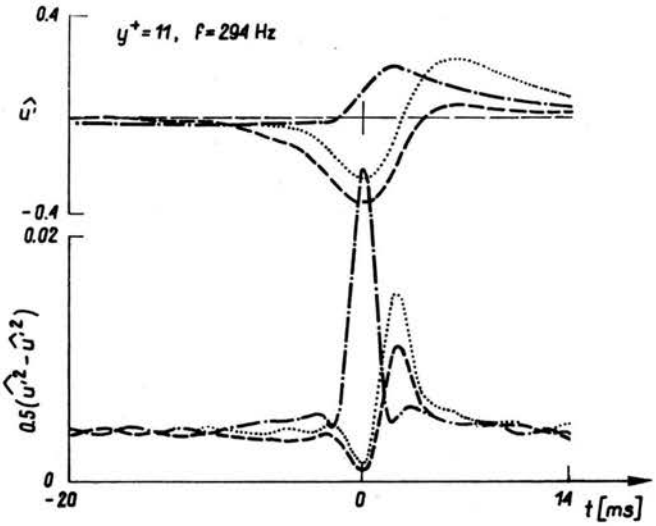

FIG. 8. Comparison between the conditionally averaged patterns obtained by different methods of detection. $y^+ = 11$, $Tu^{*2}/\nu = 10$.

····· present method, $T^+ = 2.8$, –·–·–·– Blackwelder, Kaplan (1976) method, $T^+ = 2.8$, $k = 0.38$, ——— Wilmarth, Lu (1972) method, $T^+ = 2.8$.

Detailed examination of the signal showed that all the methods did not detect the same events. For example, the Blackwelder and Kaplan method detected about 35% of events that had high frequency kinetic energy peaks occurring during the deceleration phase.

The second method of comparison (shown in Fig. 9) involved choosing threshold levels according to the recommendations of the authors concerned. The Blackwelder and Kaplan method produces now acceptable conditionally-averaged patterns. In fact the correct threshold level in this method is required to be obtained by looking at the conditionally-averaged patterns. However, at this threshold level ($k = 1.2$) the number of detected events is too small ($T^+ = 37$). It must be stated that all these detections, occurring during the acceleration phase, were accepted by the present technique as well. The conclusion that can be drawn from this is that the Blackwelder–Kaplan technique is partial to the largest events. The conditionally-averaged pattern obtained by the Willmarth–Lu technique worsened as we changed the threshold level.

4. Conclusions

The technique described in this paper by using all the information available in the signal produces reliable estimates of the mean burst interval period, which are in agreement with currently accepted values. Furthermore it shows conditionally-averaged patterns that are generally accepted for the description of coherent structures in the wall region. This twin purpose is, at present, not served by other methods.

The first author acknowledges with gratitude the financial support of a research fellowship provided by the Eindhoven University of Technology.

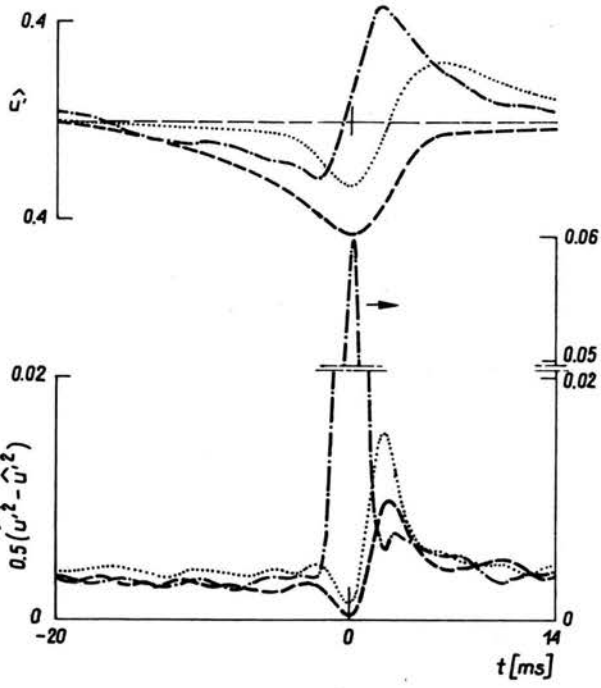

FIG. 9. Comparison between the conditionally averaged patterns obtained by different methods of detection. $y^+ = 11$, $Tu^{*2}/\nu = 10$.

····· present method, $T^+ = 2.8$, –·–·–·– Blackwelder, Kaplan (1976) method, $T^+ = 37$, $k = 1.2$, ——— Wilmarth, Lu (1972) method, $T^+ = 5.6$.

References

1. R. F. BLACKWELDER and R. E. KAPLAN, J. Fluid Mech., **76**, 89, 1976.
2. R. S. BRODKEY, J. M. WALLACE amd H. ECKELMANN, J. Fluid Mach., **63**, 209, 1974.
3. E. R. CORINO, and R. S. BRODKEY, J. Fluid Mech., **37**, 1, 1969.
4. S. S. LU and W. W. WILLMARTH, J. Fluid Mech., **60**, 481, 1973.
5. G. R. OFFEN and S. J. KLINE, J. Fluid Mech., **62**, 223, 1974.
6. K. N. RAO, R. NARASIMHA and M. A. B. NARAYANAN, J. Fluid Mech., **48**, 339, 1971.

7. M. UEDA and J. O. HINZE, J. Fluid Mech., **67**, 125, 1975.
8. A. P. VAN DE VEN, Internal report R-309-A, Laboratory for Fluid Mechanics and Heat Transfer, Dept. of Appl. Phys. Eindhoven University of Technology, 1977.
9. J. M. WALLACE, R. S. BRODKEY and H. ECKELMANN, J. Fluid Mech., **83**, 673, 1977.
10. W. W. WILLMARTH, Adv. in App. Mech., **15**, 159, 1975.
11. W. W. WILLMARTH and S. S. LU, J. Fluid Mech., **55**, 65, 1972.

TECHNICAL UNIVERSITY OF POZNAŃ, POLAND
and
EINDHOVEN UNIVERSITY OF TECHNOLOGY, EINDHOVEN, THE NETHERLANDS.

Received November 16, 1981.